Giant saturation absorption of tungsten trioxide film prepared based on the seedless layer hydrothermal method

Xiaoguang Ma(马晓光)[1,2,3], Fangzhen Hu(胡芳珍)[2,3], Xi Chen(陈希)[2,3], Yimeng Wang(王艺盟)[2,3], Xiaojian Hao(郝晓剑)[1,†], Min Gu(顾敏)[2,3,‡], and Qiming Zhang(张启明)[2,3,§]

[1] *Science and Technology on Electronic Test and Measurement Laboratory, North University of China, Taiyuan* 030051, *China*
[2] *Institute of Photonic Chips, University of Shanghai for Science and Technology, Shanghai* 200093, *China*
[3] *Centre for Artificial-Intelligence Nanophotonics, School of Optical-Electrical and Computer Engineering, University of Shanghai for Science and Technology, Shanghai* 200093, *China*

(Received 7 September 2022; revised manuscript received 14 December 2022; accepted manuscript online 30 December 2022)

Nonlinear materials have gained wide interest as saturable absorbers and pulse compression for pulsed laser applications due to their unique optical properties. This work investigates the third-order nonlinear phenomenon of tungsten trioxide (WO_3) thin films. The giant nonlinear absorption and nonlinear refractive index of WO_3 thin films were characterized by *Z*-scan method at 800 nm. We experimentally observed the giant saturable absorption (SA) and nonlinear refractive index of WO_3 thin films prepared by the seedless layer hydrothermal method, with SA coefficient being as high as -2.59×10^5 cm·GW^{-1}. The SA coefficient is at least one order of magnitude larger than those of the conventional semiconductors. The nonlinear refractive index n_2 of WO_3 film has been observed for the first time in recent studies and the corresponding coefficient can be up to 1.793 cm^2·GW^{-1}. The large third-order nonlinear optical (NLO) response enables WO_3 thin films to be promising candidates for optoelectronic and photonic applications in the near-infrared domain.

Keywords: tungsten trioxide, *Z*-scan, saturable absorption

PACS: 42.65.–k, 42.70.Nq **DOI:** 10.1088/1674-1056/acaf2a

1. Introduction

The fascinating light–matter interactions in nonlinear optical (NLO) materials have been the focus of recent optical research because of their potential for innovative applications in nanoelectronics and nanophotonics.[1] In the field of nonlinear optics, novel and promising applications such as saturable absorbers, optical switching,[2,3] mode-locking, optical limiting,[4–9] and optical bistability[10] extensively use the remarkable nonlinear properties of NLO materials. Saturable absorption (SA) is a nonlinear effect that is caused by Pauli-blocking. Namely, the excited electrons will occupy the possible states in the conduction band until all of the available states are full, and photobleaching occurs with further laser irradiation.[7] The SA phenomenon has been widely investigated in black phosphorus,[11–14] graphene,[9,15,16] transition-metal dichloride[4,5,17,18] and other NLO materials.[19] The exploration of high-performance NLO materials remains critical and has attracted considerable attention.

Recently, researchers have shown a growing interest in semiconductor materials, especially metal oxide nanoparticles, because of their giant third-order optical nonlinearity and low optical limiting threshold.[20] As a novel nonlinear material, WO_3 is desirable for the preparation of high-performance nonlinear devices due to its wide band gap and high nonlinearity. Therefore, it has a wide range of applications in laser beam shaping, saturable absorbers, mode-locking and ultrafast photonics in the nonlinear domain.[21–23] The NLO properties of three tungsten trioxide (WO_3) nanostructures (nanowires, nanoplates, and nanoclusters) were investigated via the open-aperture *Z*-scan method under nanosecond laser pulses at 532 nm. These nanostructures also exhibited an intensity-dependent transition from SA to reverse saturable absorption (RSA) with increasing laser intensity.[24] The optical limiting of WO_3 nanoparticles in nanosecond laser pulses at 1064 nm was studied, demonstrating that nanoscale WO_3 has higher optical power limiting than its micronsized counterpart.[25] Various techniques have been successfully developed to fabricate nanostructured WO_3 films, including anodic oxidation,[26] electrodeposition,[27,28] sol-gel methods,[29,30] magnetron sputtering,[31] and hydrothermal methods.[32,33] Moreover, it is worth mentioning that the optical nonlinear response characterized by the different preparation methods of the films is relatively different. In general, a seed layer is required for the growth of WO_3 nanostructures prepared by hydrothermal methods directly on conducting substrates. This crystal-seed-assisted hydrothermal process generally involves a rather complex process to prepare the seed layer. In addition, the seed layer can lengthen the electron transport path, resulting in a slow response rate.[34] In this regard, WO_3 films based on the seedless layer hydrothermal

†Corresponding author. E-mail: haoxiaojian@nuc.edu.cn
‡Corresponding author. E-mail: gumin@usst.edu.cn
§Corresponding author. E-mail: qimingzhang@usst.edu.cn

© 2023 Chinese Physical Society and IOP Publishing Ltd

method have been recently reported.[34] However, the nonlinearity of the films prepared by this method has not been reported so far.

In this work, we investigated the third-order nonlinear optical response of WO_3 films with a femtosecond laser at the wavelength of 800 nm via the *Z*-scan method. Moreover, we experimentally observed the giant SA of WO_3 films prepared by the seedless layer hydrothermal method. And the SA coefficient was one to two orders of magnitude higher than the highest value previously reported.[35,36] Moreover, the positive nonlinear refractive index n_2 of WO_3 film was observed for the first time in recent investigations. In conclusion, our study not only observes a large nonlinear absorption coefficient in a simple preparation method but also paves the way for the integration of functionalized optoelectronic and photonic devices.[37–39]

2. Experimental details

2.1. Materials and characterization

All chemicals involved in the experiment were of analytical grade with no further purification, which were purchased from Sinopharm Chemical Reagent Co. Ltd (China). The FTO glasses used in this work were treated with sequential sonication in acetone, ethanol and deionized water for 15 min to ensure the flatness of the prepared films.

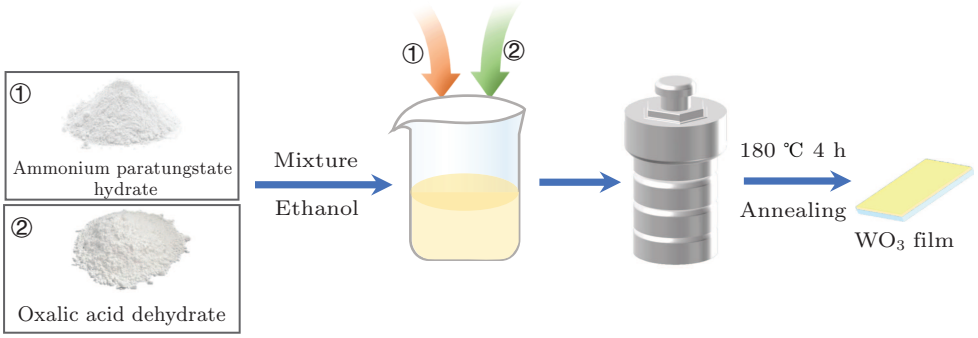


Fig. 1. Flow chart of WO_3 film preparation based on seed-layer-free hydrothermal method.

The WO_3 films were grown directly on the FTO substrate using a simple hydrothermal method without a seed layer. As shown in Fig. 1, the films were acquired by a prototypical hydrothermal process. The precursor solution for hydrothermal use was prepared by dissolving 0.3042 g of ammonium paratungstate hydrate ($H_{40}N_{10}O_{41}W_{12} \cdot xH_2O$, molecular weight 3042) and 6.3 g of oxalic acid dehydrate ($C_2H_2O_4{\cdot}2H_2O$) in 40 g of ethanol. The resulting mixture was sonicated for 15 min and then transferred to a 50 ml teflon-lined stainless steel autoclave. A piece of FTO glass was placed in the autoclave against the wall with the conductive side facing down. Then it was sealed in the autoclave and remained at 180 °C for 4 hours and annealed in a fume hood until completely cooled. Finally, WO_3 films were obtained by washing the synthesized films with ethanol and then drying the films in the air.

2.2. The *Z*-scan measurement

The nonlinear optical properties of the WO_3 films were characterized by *Z*-scan measurements using a femtosecond laser with a central wavelength of 800 nm, a pulse duration of 120 fs, and a pulse repetition frequency of 5 kHz. A half-wave plate together with a linear polarizer was exploited to vary the input laser power. The well-prepared sample was placed perpendicular to the beam axis and translated along the *Z*-axis on a linear motorized stage. A photomultiplier tube (Thorlabs, PMM02) was used to monitor the power.

3. Results and discussion

Figure 2(a) shows the 3D surface morphology of the WO_3 film characterized in the region of 17.2 μm×17.2 μm by atomic force microscopy (AFM, CSPM5500, China). The plan-view SEM image and cross-sectional view of the WO_3 film are shown in Figs. S1 and S2 in the supporting information, respectively. The average thickness of the as-prepared film is about 1.664 μm. Figure 2(b) presents the Raman spectrum of the thin WO_3 film. The raw films show sharp resonance peaks centered at 250 cm^{-1}, 700 cm^{-1}, and 790 cm^{-1}. The bands at 700 cm^{-1} and 790 cm^{-1} are derived from the W–O–W stretching vibrations of the bridging oxygen atoms, while the Raman band in the range of 250 cm^{-1} can be associated with the W–O bending vibrations of WO_3.[40,41] To investigate the linear optical properties and optical band gap, the absorption spectrum of the WO_3 films from 260 nm to 1200 nm is shown in Fig. 2(c). It can be seen that the optical absorption intensity decreases significantly as the wavelength increases from ultraviolet (UV) to near-infrared (NIR). The calculated Tauc plot in Fig. 2(d) implies that the WO_3 film has a bandgap of about 2.2 eV.

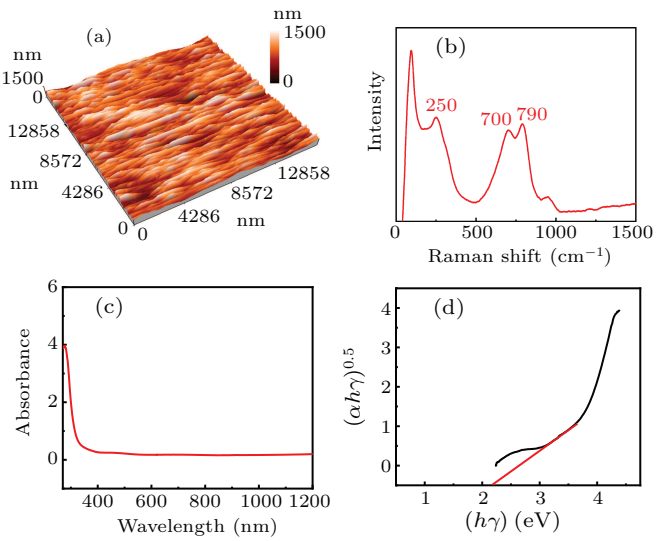


Fig. 2. Characterization of WO_3 films grown via hydrothermal method. (a) 3D surface morphology characterized by atomic force microscopy. (b) Raman spectrum of WO_3 film. (c) Absorbance spectrum and (d) Tauc plot of the WO_3 film.

To investigate the third-order nonlinear optical properties of WO_3, we characterized the nonlinear absorption and nonlinear refraction of the prepared WO_3 films at the wavelength of 800 nm using the Z-scan technique. The open-aperture (OA) and close aperture (CA) Z-scan are employed to study the nonlinear optical response of the WO_3 film. The position-dependent transmittance can be defined as a function of the sample position on the Z-axis. Herein, we performed the measurements of OA and CA Z-scan at the power intensity of 39.9 MW/cm^2, as illustrated in Figs. 3(a) and 3(b). The transmittance shows a positive variation in Fig. 3(a), indicating a typical SA phenomenon, since the electrons are fermions and must obey the Pauli-blocking principle.[42] For CA Z-scan, it exhibits a distinct valley-peak configuration, indicating that the WO_3 film has a positive nonlinear refractive index n_2 (self-focusing), as illustrated in Fig. 3(b). To avoid the effect of material degradation on the results, Z-scan measurements were carried out using low laser intensities. Afterward, the Z-scan results at low laser intensities will be examined again to ensure that there are no differences from the previous measurements.

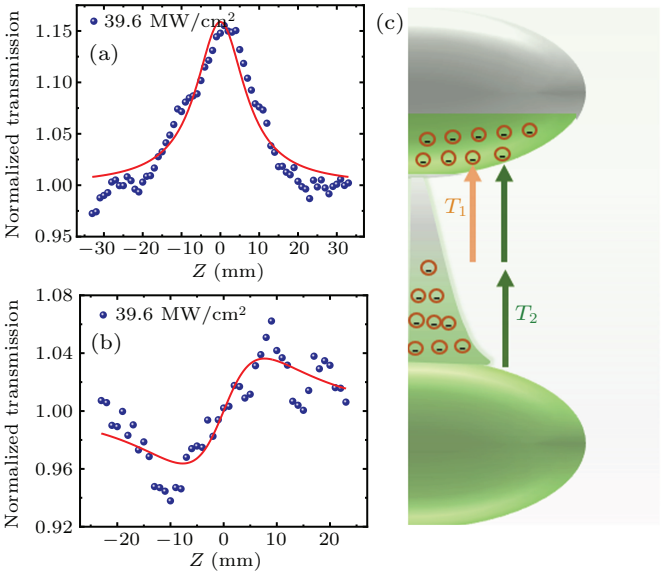


Fig. 3. (a) Open aperture Z-scan scatters of WO_3 film fitted with theory at a power intensity of 39.6 MW/cm^2 (red solid lines).[6] (b) Close aperture Z-scan scatters of WO_3 film fitted with theory at a power intensity of 39.6 MW/cm^2 (red solid lines). (c) The absorption process for laser radiation at a wavelength of 800 nm.

Table 1. A comparison of nonlinear saturable absorption coefficients of WO_3 film with that of other nanomaterials.

Material	Laser param	Thickness	β (cm/GW)	
MoO_3 dispersion	1550 nm/	1 mm	-1.2×10^{-3}	[45]
BP dispersion	532 nm/6 ns	1 mm	-2.85×10	[46]
BP dispersion	1064 nm/6 ns	1 mm	-9.17×10	[46]
Nb_2C film	1064 nm/10 ps	10–15 nm	-1.0×10^5	[47]
GeP film	1030 nm/13 ps	80 μm	-9.9×10	[48]
InSe film	1064 nm/15 ps	–	-1.9×10^3	[49]
$PdSe_2$ film	500 nm/190 fs	20 nm	-4.13×10^4	[50]
GO dispersion	790 nm/80 fs	1 mm	-4.4×10	[51]
rGO	800 nm/120 fs	1200 nm	-4.6×10^4	[52]
MoS_2 dispersion	532 nm/4 ns	2 mm	-1.2×10	[43]
MoS_2 dispersion	1064 nm/4 ns	2 mm	-1.5	[43]
D-WO_3 dispersion	532 nm/4 ns	2 mm	-6.7	[43]
D-WO_3 dispersion	1064 nm/4 ns	2 mm	-8.8	[43]
WO_3 nanowires	532 nm/7 ns	–	-2.5	[26]
WO_3 nanoplates	532 nm/7 ns	80 nm	-3	[26]
WO_3 nanoflower clusters	532 nm/7 ns	–	-1.9	[26]
WO_3 film	800 nm/120 fs	–	-2.59×10^5	this work

The normalized transmittance is 115.8% at a focusing intensity of 39.9 MW/cm^2. To further elaborate on magnitude of the nonlinear response of the WO_3 film, the absolute value of nonlinear SA coefficients β and nonlinear refractive index n_2 were fitted and calculated to be 2.59×10^5 cm·GW^{-1} and 1.793 cm^2·GW^{-1} by fitting the OA and CA Z-scan curves at representative power intensity of 39.9 MW/cm^2. As summarized in Table 1, the giant nonlinear SA coefficient of the WO_3

film is at least two orders of magnitude larger than those of the conventional semiconductors,[2,36,43] implying that such WO_3 film has the potential to be a high-performance saturable absorber for passively mode-locked and Q-switched lasers. To the best of our knowledge, the nonlinear refractive index n_2 of the WO_3 film is measured for the first time in recent investigations.

To elucidate the possible mechanisms of the WO_3 film nonlinearity, we will proceed with the following discussion. In theory, the nonlinear optical (NLO) response of a material may stem from state filling (SF), free carrier absorption (FCA), or two-photon absorption (TPA) (or multiphoton absorption (MPA)), which depends on the wavelength of the applied laser and the band gap of the material. RSA can be associated with TPA, MPA, or FCA, while SF will induce SA. In our case, the main reason is that laser excitation of the sample is accompanied by interband transition of electrons through absorption of photons.[42,44] The possible electron transfer process of the WO_3 film is illustrated in Fig. 3(c). Intriguingly, the absorption spectrum suggests that the optical bandgap energy of pristine WO_3 film is 2.2 eV. For the 800 nm laser irradiation, although the double of photon energy is greater than the optical bandgap, but TPA has not been observed experimentally, implying that the TPA process from the valence band to the conduction band is relatively weak at the wavelength of 800 nm. This case is similar to the investigation reported by Hou and co-workers.[36]

4. Conclusion and perspectives

In conclusion, we investigated the nonlinear absorption of WO_3 films at 800 nm wavelength of femtosecond laser via the Z-scan method. To the best of our knowledge, this is the first observation of SA phenomenon in WO_3 films prepared using the seedless layers hydrothermal method. We experimentally observed that the giant SA of WO_3 films, with the SA coefficient being as high as -2.59×10^5 cm·GW^{-1}, is at least one order of magnitude larger than those of the conventional semiconductors. Moreover, the sample exhibits SA behavior, the main reason may be due to the band-filling effect, that is, the interband transition of electrons through the absorption of photons. The nonlinear refractive index n_2 of WO_3 film has been observed for the first time in recent studies and the corresponding coefficient can be up to 1.793 cm^2·GW^{-1}. Our results not only exhibit a giant SA coefficient of WO_3 film under a simple and convenient preparation method but also pave the way for the integration of functionalized optoelectronic and photonic devices.

Acknowledgements

We would like to acknowledge the support from the Science and Technology Commission of Shanghai Municipality (Grant No. 21DZ1100500), the Shanghai Municipal Science and Technology Major Project, the Shanghai Frontiers Science Center Program (2021–2025 No. 20), the National Key Research and Development Program of China (Grant No. 2021YFB2802000), the National Natural Science Foundation of China (Grant No. 61975123), the National Natural Science Foundation of China (Grant No. 52075504), and Fund for Shanxi '1331Project' Key Subject Construction and Shanxi Doctor Innovation Project (2019).

References

[1] Bonaccorso F, Sun Z, Hasan T and Ferrari A C 2010 *Nat. Photon.* **4** 611
[2] Guo Q B, Cui Y D, Yao Y H, Ye Y T, Yang Y, Liu X M, Zhang S A, Liu X F, Qiu J R and Hosono H 2017 *Adv. Mater.* **29** 1700754
[3] Hayat A, Nevet A, Ginzburg P and Orenstein M 2011 *Semicond. Sci. Technol.* **26** 083001
[4] Dong N N, Li Y X, Zhang S F, McEvoy N, Zhang X Y, Cui Y, Zhang L, Duesberg G S and Wang J 2016 *Opt. Lett.* **41** 3936
[5] Dong N N, Li Y X, Zhang S F, McEvoy N, Gatensby R, Duesberg G S and Wang J 2018 *ACS Photon.* **5** 1558
[6] Jia L N, Wu J Y, Yang T S, Jia B H and Moss D J 2020 *ACS Appl. Nano Mater.* **3** 6876
[7] Wang Y D, Wang Y W, Chen K Q, Qi K, Xue T Y, Zhang H, He J and Xiao S 2020 *ACS Nano* **14** 10492
[8] Guo J, Wang Z H, Shi R C, Zhang Y, He Z W, Gao L F, Wang R, Shu Y Q, Ma C Y, Ge Y Q, Song Y F, Fan D Y, Xu J L and Zhang H 2020 *Adv. Opt. Mater.* **8** 2000067
[9] Demetriou G, Bookey H T, Biancalana F, Abraham E, Wang Y, Ji W and Kar A K 2016 *Opt. Express* **24** 13033
[10] Wang Z Q, Cai B Y, Wan Z F, Zhang Y Y, Ma X G, Gu M and Zhang Q M 2022 *Nanomaterials* **12** 1117
[11] Yang T S, Abdelwahab I, Lin H, Bao Y, Rong Tan S J, Fraser S, Loh K P and Jia B H 2018 *ACS Photon.* **5** 4969
[12] Chen Y, Jiang G B, Chen S Q, Guo Z N, Yu X F, Zhao C J, Zhang H, Bao Q L, Wen S C, Tang D Y and Fan D Y 2015 *Opt. Express* **23** 12823
[13] Wang Y W, Huang G H, Mu H R, Lin S H, Chen J Z, Xiao S, Bao Q L and He J 2015 *Appl. Phys. Lett.* **107** 091905
[14] Lee, S Y, Kim Y H, Cho S M, Kim G H, Kim T Y, Ryu H, Kim H N, Kang H B, Hwang C Y and Hwang C S 2017 *Sci. Rep.* **7** 41152
[15] Bao Q L, Zhang H, Wang B, Ni Z H, Lim C H Y X, Wang Y, Tang D Y and Loh K P 2011 *Nat. Photon.* **5** 411
[16] Bao Q L, Zhang H, Wang Y, Ni Z H, Yan Y L, Shen Z X, Loh K P and Tang D Y 2009 *Adv. Funct. Mater.* **19** 3077
[17] Zhang H, Lu, S B, Zheng J, Du J, Wen S C, Tang D Y and Loh K P 2014 *Opt. Express* **22** 7249
[18] Chen H, Liu T J, Su Z Q, Shang L and Wei G 2018 *Nanoscale. Horiz.* **3** 74
[19] Wang Y W, Liu S, Yuan J, Wang P, Chen J Z, Li J B, Xiao S, Bao Q L, Gao Y L and He J 2016 *Sci. Rep.* **6** 33070
[20] Li Y, Zhang Z and Zhu J H 2021 *Opt. Mater.* **119** 111359
[21] Chen Z D, Wang Y G, Lu L, Lv R D, Wei L L, Liu S C, Wang J and Wang X 2018 *Chin. Phys. B* **27** 084206
[22] Li Y C, Ge C, Wang P, Liu S, Ma X R, Wang B, Song H Y and Liu S B 2022 *Chin. Phys. B* **31** 067102
[23] Luo Z C, Liu M, Luo A P and Xu W C 2018 *Chin. Phys. B* **27** 094215
[24] Huang D D, Zheng C, Li W, Guo Q H and Chen W Z 2019 *Opt. Mater.* **88** 451
[25] Muller O and Gibot P 2019 *Opt. Mater.* **95** 109220
[26] Ou J Z, Balendhran S, Field M R, McCulloch D G, Zoolfakar A S, Rani R A, Zhuiykov S, O'Mullaneb A P and Kalantar-zadeh K 2012 *Nanoscale* **4** 5980
[27] Liu L, Layani M, Yellinek S, Kamyshny A, Ling H, Lee P S, Magdassi S and Mandler D 2014 *J. Mater. Chem. A* **2** 16224
[28] Zhu T, Chong M N and Chan E S 2014 *Chemsuschem* **7** 2974
[29] Lia C P, Lin F, Richards R M, Engtrakul C, Tenent R C and Wolden C A 2014 *Sol. Energy Mater. Sol. Cells* **121** 163

[30] Patrocinio A O T, Paula L F, Paniago R M, Freitag J and Bahnemann D W 2014 *ACS Appl. Mater. Interfaces* **6** 16859

[31] Sauvet K, Sauques L and Rougier A 2009 *Sol. Energy Mater. Sol. Cells* **93** 2045

[32] Wang J M, Khoo E, Lee P S and Ma J 2009 *J. Phys. Chem. C* **113** 9655

[33] Chen Z, Peng Y T, Liu F, Le Z Y, Zhu J, Shen G R, Zhang D Q, Wen M C, Xiao S N, Liu C P, Lu Y F and Li H X 2015 *Nano Lett.* **15** 6802

[34] Ma D, Li T, Xu Z, Wang L and Wang J 2018 *Sol. Energy Mater. Sol. Cells* **177** 51

[35] Li H, Hou R P, Sun Y H, Diao M J, Liang Y, Chen X, Huang Z P, Wang J, Humphrey M G, Yu Z Y and Zhang C 2021 *Adv. Opt. Mater.* **9** 2002188

[36] Hou R P, Li H, Diao M J, Sun Y H, Liang Y, Yu Z Y, Huang Z P and Zhang C 2022 *Nano Res.* **15** 326

[37] Goi E, Zhang Q M, Chen X, Luan H T and Gu M 2020 *PhotoniX* **1** 3

[38] Chen M, Wan Z F, Dong H, Chen Q Y, Gu M and Zhang Q M 2022 *Natl. Sci. Open* **1** 20220020

[39] Zhang Q M, Yu H Y, Barbiero M, Wang B K and Gu M 2019 *Light: Sci. Appl.* **8** 42

[40] Pyper O, Kaschner A and Thomsen C 2002 *Sol. Energy Mater. Sol. Cells* **71** 511

[41] Luo J Y, Zhou Y Y, Huang D, Zeng Q G and Wang Y 2012 *Adv. Mater. Res.* **529** 69

[42] Chen X, Huang J W, Chen C D, Chen M L, Hu G H, Wang H Q, Dong N N and Wang J 2022 *Adv. Opt. Mater.* **10** 2101963

[43] Zhai X P, Gao L F, Zhang H, Peng Y, Zhang X D, Wang Q and Zhang H L 2022 *ACS Appl. Nano Mater.* **5** 1169

[44] Yu J, Kuang X F, Li J Z, Zhong J H, Zeng C, Cao L K, Liu Z W, Zeng Z X S, Luo Z Y, He T C, Pan A L and Liu Y P 2021 *Nat. Commun.* **12** 1083

[45] Lin J M, Chen H L, Ma D T, Gong Y N, Li Z J, Li D L, Song Y F, Zhang F, Li J Q, Wang H C, Zhang Y P and Zhang H 2020 *Nanoscale* **12** 23140

[46] Huang J W, Dong N N, Zhang S F, Sun Z Y, Zhang W H and Wang J 2017 *ACS Photonics* **4** 3063

[47] Li G R, Liu J T, Wang F F, Nie H K, Wang R H, Yang K J, Zhang B T and He J L 2021 *Adv. Mater. Interfaces* **8** 2001805

[48] Yu T T, Nie H K, Wang S P, Zhang B T, Zhao S Q, Wang Z M, Qiao J, Han B, He J L and Tao X T 2019 *Adv. Opt. Mater.* **8** 1901490

[49] Pan H, Cao L H, Chu H W, Wang Y C, Zhao S Z, Li Y, Qi N, Sun Z L, Jiang X T, Wang R, Zhang H and Li D C 2019 *ACS Appl. Mater. Interfaces* **11** 48281

[50] Ye C Y, Yang Z Q, Dong J H, Huang Y F, Song M M, Sa B S, Zheng J Y and Zhan H B 2021 *Small* **17** 2103938

[51] Kumar S, Anija M, Kamaraju N, Vasu K S, Subrahmanyam K S, Sood A K and Rao C N R 2009 *Appl. Phys. Lett.* **95** 191911

[52] Ma X G, Wang Y M, Hao X J, Gu M and Zhang Q M 2022 *Adv. Mater. Interfaces* **9** 2200890